Validation of highly selective Sphingosine kinase 2 inhibitors SLM6031434 and HWG-35D as effective anti-fibrotic treatment options in a mouse model of tubulointerstitial fibrosis.

Stephanie Schwalm[1]*, Sandra Beyer[1], Redona Hafizi[5], Sandra Trautmann[2], Gerd Geisslinger[2], David R. Adams[3], Susan Pyne[4], Nigel Pyne[4], Liliana Schaefer[1], Andrea Huwiler[5#] and Josef Pfeilschifter[1#]

[1]Pharmazentrum Frankfurt/ZAFES, Institute of General Pharmacology and Toxicology, Universitätsklinikum and Goethe-Universität Frankfurt, Theodor-Stern-Kai 7, 60590 Frankfurt am Main, Germany.

[2]Pharmazentrum Frankfurt/ZAFES, Institute of Clinical Pharmacology, Universitätsklinikum and Goethe-Universität Frankfurt, Theodor-Stern-Kai 7, 60590 Frankfurt am Main, Germany.

[3] School of Engineering & Physical Sciences, Heriot-Watt University, Edinburgh, U.K.

[4]Strathclyde Institute of Pharmacy and Biomedical Sciences, University of Strathclyde, Glasgow, U.K.

[5]Institute of Pharmacology, University of Bern, Inselspital INO-F, CH-3010 Bern, Switzerland.

[#] shared last-authorship

Address for correspondence:

Dr. Stephanie Schwalm

Universitätsklinikum der Goethe-Universität Frankfurt

Theodor-Stern-Kai 7

D-60590 Frankfurt am Main, Germany

Phone: +49-69-63016963

Fax: +49-69-63017942

Email: S.Schwalm@med.uni-frankfurt.de

Abstract

Renal fibrosis is characterized by chronic inflammation and excessive accumulation of extracellular matrix and progressively leads to functional insufficiency and even total loss of kidney function. In this study we investigated the anti-fibrotic potential of two highly selective and potent SK2 inhibitors, SLM6031434 and HWG-35D, in unilateral ureter obstruction, a model for progressive renal fibrosis, in mice. In both cases, treatment with SLM6031434 or HWG-35D resulted in an attenuated fibrotic response to UUO in comparison to vehicle-treated mice as demonstrated by reduced collagen accumulation and a decreased expression of collagen-1 (Col1), fibronectin-1 (FN-1), connective tissue growth factor (CTGF), and α-smooth muscle actin (α-SMA). Similar to our previous study in *Sphk2*$^{-/-}$ mice, we found an increased protein expression of Smad7, a negative regulator of the pro-fibrotic TGFβ/Smad signaling cascade, accompanied by a strong accumulation of sphingosine in SK2 inhibitor-treated kidneys. Treatment of primary renal fibroblasts with SLM6031434 or HWG-35D dose-dependently increased Smad7 expression and ameliorated the expression of Col1, FN-1 and CTGF.

In summary, these data prove the anti-fibrotic potential of SK2 inhibition in a mouse model of renal fibrosis, thereby validating SK2 as pharmacological target for the treatment of fibrosis in chronic kidney disease.

Keywords: SK2 inhibition, SLM6031434, HWG-35D, CTGF, Collagen I, tubulointerstitial fibrosis, fibroblasts

Introduction

Renal fibrosis is a final common feature of chronic kidney disease (CKD) irrespective of the initiating disease trigger for this broad and variable illness category. It is characterized by a massive deposition of extracellular matrix (ECM) in the kidney parenchyma leading to tissue scarring, functional insufficiencies and finally end-stage renal disease and kidney failure demanding renal replacement therapy (RRT). In the worldwide ranking of leading causes for a reduced life expectancy, a recent global forecasting study predicted a dramatic shift for chronic kidney disease from rank 16th (2016) to rank 5th in 2040 [1], which will result in an enormous increase of morbidity costs for dialysis or kidney transplantation. Since there are still no therapeutic options for the treatment of renal fibrosis in CKD available, we urgently need to identify new anti-fibrotic treatment targets to reduce the burden of this global public health problem.

Sphingolipids are important components of cellular membranes but have also been shown to regulate a myriad of important cell responses, such as cell proliferation, survival, apoptosis, and migration, thereby governing complex functions such as vascular integrity, angiogenesis and inflammation [2,3]. It is well established that sphingolipid-derived mediators, especially sphingosine 1-phosphate (S1P) influence fibrotic events in various organs, including lung, liver, heart, skin and kidney [4–6]. S1P acts in a profibrotic manner by cross-activating the transforming growth factor (TGF) β/Smad signalling cascade *via* the extracellular activation of specific G-protein coupled S1P receptors, of which five receptor subtypes have been identified [7]. Two sphingosine kinases (SK1 and SK2) produce S1P by phosphorylating sphingosine in an ATP dependent manner. Although both enzymes generate S1P and show a ubiquitous expression pattern, they differ in subcellular localization and biochemical properties such as substrate selectivity, suggesting different functions of the two isoforms [8]. SK1 is the more intensively studied isoform and has been shown to be induced by the key profibrotic mediator TGFβ and is upregulated in various kidney disease models, such as tubulointerstitial fibrosis [9], diabetic nephropathy [10] and polycystic kidney disease [11]. However, SK1 depletion by using genetic knockout (*Sphk1*$^{-/-}$) mice or pharmacological inhibition

in these animal models resulted in aggravated disease severity with more impaired renal function, increased fibrosis and exacerbated cystogenesis [9–11], pointing to a protective role for SK1. It has been shown that SK1 upregulation enhances the levels of intracellular S1P levels, which in contrast to extracellular S1P, downregulates the expression of the profibrotic marker protein connective tissue growth factor (CTGF) by yet unidentified mechanisms [10].

More recent studies have started to investigate the role of SK2 in renal pathologies, and have shown that SK2 is expressed in tubuli and in the renal interstitium [12,13]. Our group demonstrated that SK2 protein and activity is strongly upregulated in fibrotic renal tissue. Unlike SK1, SK2 plays a profibrotic role, since SK2-deficient mice showed ameliorated kidney fibrosis compared to wildtype mice in a model of unilateral ureteral obstruction (UUO) [12]. The reduced expression of profibrotic markers such as collagen-1 (Col1), fibronectin-1 (FN1) and CTGF in ligated *Sphk2*$^{-/-}$ kidneys was associated with an upregulation of Smad7, an important inhibitor of the profibrotic TGFβ/Smad signaling cascade. Smad7 upregulation could be mimicked by stimulation of primary cultures of murine renal fibroblasts with sphingosine, a sphingolipid which strongly accumulated in *Sphk2*$^{-/-}$ renal tissue. The profibrotic role of SK2 was confirmed in a complementary approach using mice overexpressing human SK2. These mice developed a more severe fibrotic response in obstructed kidneys, and showed reduced Smad7 levels [12]. A protective effect of SK2 depletion was also confirmed in models of folic-acid induced nephropathy and unilateral ureter ischemia/reperfusion-induced renal injury and fibrosis [14,15].

In the present study, we investigated the therapeutic potential of two relatively new selective SK2 inhibitors, SLM6031434 and HWG-35D (compound 55 [16]) on tubulointerstitial fibrosis induced by unilateral ureter ligation (UUO) in mice. We demonstrate that, similar to a genetic SK2 depletion, treatment with SLM or HWG-35D attenuated the UUO-induced fibrotic response compared to vehicle treatment. Furthermore, SK2 inhibition led to sphingosine accumulation and Smad7 upregulation in obstructed kidneys and primary cultures of mouse renal fibroblasts. Taken

together, we have positively validated two highly selective and potent pharmacological inhibitors of SK2 and shown their beneficial effect on renal fibrosis.

Materials and Methods

SK2 inhibitor treatment (SLM6031434, HWG-35D) in mice

SLM6031434 and HWG-35D, dissolved in 20 % hydroxy-propyl-β-cyclodextrine/PBS (AppliChem GmbH, Darmstadt, Germany), or vehicle solution alone were intraperitoneally administered to mice daily starting two days prior to UUO induction until the end of the experiment (9 days in total).

Unilateral ureteral obstruction model

The unilateral ureteral obstruction model was performed in adult male 10-12 weeks old mice as previously described [12]. Briefly, under ketamin/xylazin induced anesthesia (200 mg/10 mg/kg) and after a left flank incision, the ureter was exposed and double-ligated using 6-0 prolene ® (Ethicon, Norderstedt, Germany). Thereafter, the incision was closed under aseptic conditions. The contralateral kidney served as a control. Kidneys were harvested 7 days after ligation and either snap frozen in liquid nitrogen or fixed in buffered formalin. All procedures were conducted in accordance with the German Animal Protection Act and were approved by the Ethics Review Committee for laboratory animals of the District Government of Darmstadt, Germany.

Chemicals and materials

TGFβ and antibodies against fibronectin-1 and α-SMA were from Sigma-Aldrich,Taufkirchen, Germany; SLM60314343 was purchased from Tocris (Bio-Techne GmbH, Wiesbaden, Germany); HWG-35D was synthesized and characterized as previously described [16]; the Collagen1 antibody was from Merck Millipore, Darmstadt, Germany; GAPDH was from GeneTex, Irvine, CA, USA; CTGF (L-20) and Smad7 (B-8) antibodies were from Santa Cruz Biotechnology, Heidelberg, Germany; all cell culture nutrients were from Life Technologies, Karlsruhe, Germany.

Renal histology and immunohistochemistry

Paraffin-embedded renal sections (3 µM) were deparaffinized and stained by periodic acid-Schiff reaction (PAS). AZAN trichrome and Sirius Red staining for detection of interstitial collagen was performed as previously described [12]. For immunohistochemical stainings, sections were incubated with anti-alpha smooth muscle actin (clone 1A4, alkaline phosphatase-labeled, Sigma-Aldrich) or F4/80 (macrophage marker, clone Cl:A3-1; Bio-Rad Laboratories GmbH, München, Germany) overnight at 4°C. Permanent AP Red Kit (Zytomed Systems) or diaminobenzidine (DAB, Vector-Laboratories, Burlingame, CA) were used for visualization and counterstaining was performed with Mayer´s hematoxylin. PAS, AZAN, αSMA and F4/80 stained sections were evaluated with an Olympus BX60 Microscope, and Sirius Red stained sections with an Axiovert 200 microscope (Zeiss, Germany) at 20x, additionally using a polarization filter. Images were acquired using an Olympus DP70 camera and examined by a blinded observer. Collagen content of the Sirius Red images was evaluated using Image J software (ImageJ, U. S. National Institutes of Health, Bethesda, Maryland, USA) of 8 – 12 randomly selected non-overlapping fields avoiding large vessels, by setting a fixed background intensity threshold and calculating unmasked pixels above threshold relative to total pixels. F4/80 positive area was evaluated using the Fuji plugin of ImageJ software version 1.51k of 4-8 randomly selected non-overlapping fields, by using the color deconvolution for DAB-hematoxylin. The brown images of F4/80 staining and αSMA were converted to an eight-pixel black/white image, followed by setting a fixed background intensity threshold and calculating unmasked pixels above threshold relative to total pixels.

Cell culture, siRNA transfection and stimulation

Primary mouse renal fibroblasts were isolated from C57BL/6 mice and cultured as previously described [17]. For stimulation, cells were starved for 24 h in serum-free medium containing 0.1 % bovine serum albumin (BSA) and were stimulated as indicated.

157 *RNA extraction and quantitative real-time PCR analysis*

158 Kidney samples frozen in liquid nitrogen were homogenized in a Micro-Dismembrator S (Sartorius
159 Stedim Biotech GmbH) (setting 3000 rpm for 30 s) and resuspended in 1 mL of TRIZOL™ reagent
160 (Sigma-Aldrich, Steinheim, Germany) for total RNA extraction according to the manufacturer's
161 protocol and used for reverse transcriptase polymerase chain reaction (RT-PCR; RevertAid™ first
162 strand cDNA synthesis kit, Thermo Fisher Scientific, Waltham, MA, USA) utilizing a random
163 hexamer primer for amplification. Real-time qPCR (TaqMan®) was performed using the Applied
164 Biosystems 7500 Fast Real-Time PCR System. TaqMan® gene expression assays and qPCR Low
165 Rox Mix were from Life Technologies (Darmstadt, Germany). The following TaqMan® gene
166 expression assays were used: murine connective tissue growth factor: Mm01192933_g1; murine
167 collagen 1a1: Mm00801666_g1; murine collagen 3a1: Mm1254476_m1, murine fibronectin-1:
168 Mm01256744_m1, murine acta-2: Mm00725412_s1, murine interferon-γ: , murine iNOS:
169 Mm01309897_m1, murine Mcr1: Mm01329362_m1 (Life Technologies, Darmstadt, Germany).
170 The threshold cycle (C_t) was calculated by the instrument's software (7500 Fast System SDS
171 Software version 1.4). Analysis of the relative mRNA expression was performed using the $\Delta\Delta C_t$
172 method. Eukaryotic 18S ribosomal RNA: Hs99999901_s1 or mouse GAPDH: 4352339E (Life
173 Technologies, Darmstadt, Germany) was used for normalisation.
174
175 *Western blot analysis*

176 Kidney or cell homogenates were prepared in lysis buffer (50 mM Tris-HCl, pH 7.4, 150 mM NaCl,
177 10% glycerol, 1% Triton X100, 2 mM EDTA, 2 mM EGTA, 40 mM β-glycerophosphate, 50 mM
178 sodium fluoride). Equal amounts of protein were separated by SDS-PAGE, transferred to
179 nitrocellulose membrane and subjected to Western blot analysis using antibodies as indicated in
180 the figure legends.
181
182

LC-MS/MS analysis of sphingolipids

The quantitation of sphingolipids was performed for tissue and plasma. Tissue pieces were homogenized with water using a swing mill (Retsch, Haan, Germany) with 4 zirconium oxide grinding balls for each sample (25Hz for 2.5 minutes) to obtain a tissue suspension of 0.05 mg/µL. 20 µL tissue homogenate (in total 1 mg tissue) or 10 µL plasma were mixed with 150 µL of water, 150 µL of extraction buffer (citric acid 30 mM, disodium hydrogen phosphate 40 mM) and 20 µL of the internal standard solution containing sphingosine-d7, sphinganine-d7 (200 ng/mL each), sphingosine-1-phosphate-d7 (all Avanti Polar Lipids, Alabaster, USA) (400 ng/mL methanol each). The mixture was extracted once with 1000 µL methanol/chloroform/hydrochloric acid (15:83:2, v/v/v). The lower organic phase was evaporated at 45 °C under a gentle stream of nitrogen and reconstituted in 100 µL of tetrahydrofuran/water (9:1, v/v) with 0.2% formic acid and 10 mM ammonium formate. Afterwards, amounts of sphingolipids were analyzed by liquid chromatography coupled to tandem mass spectrometry (LC-MS/MS). An Agilent 1100 series binary pump (Agilent technologies, Waldbronn, Germany) equipped with a Luna C8 column (150 mm x 2 mm ID, 3 µm particle size, 100 Å pore size; Phenomenex, Aschaffenburg, Germany) was used for chromatographic separation. The column temperature was 35 °C. The HPLC mobile phases consisted of water with 0.2% formic acid and 2 mM ammonium formate (mobile phase A) and acetonitrile/isopropanol/acetone (50:30:20, v/v/v) with 0.2% formic acid (mobile phase B). For separation, a gradient program was used at a flow rate of 0.3 mL/min. The initial buffer composition 55% (A)/45% (B) was held for 0.7 min and then within 4.0 min linearly changed to 0% (A)/100% (B) and held for 13.3 min. Subsequently, the composition was linearly changed within 1.0 min to 75% (A)/25% (B) and then held for another 2.0 min. The total running time was 21 min and the injection volume was 15 µL. To improve ionization, acetonitrile with 0.1% formic acid was infused post-column using an isocratic pump at a flow rate of 0.15 mL/min. After every sample, sample solvent was injected for washing the column with a 12 min run. The MS/MS analyses were performed using a triple quadrupole mass spectrometer API4000 (Sciex, Darmstadt, Germany)

equipped with a Turbo V Ion Source operating in positive electrospray ionization mode. The MS parameters were set as follows: Ionspray voltage 5500 V, source temperature 500 °C, curtain gas 30 psi, collision gas 12 psi, nebulizer gas 40 psi and heating gas 60 psi. The analysis was done in Multiple Reaction Monitoring (MRM) mode with a dwell time of 20 ms for all analytes.

Data Acquisition was done using Analyst Software V 1.6 and quantification was performed with MultiQuant Software V 3.0 (both Sciex, Darmstadt, Germany), employing the internal standard method (isotope dilution mass spectrometry). Variations in accuracy of the calibration standards were less than 15% over the whole range of calibration, except for the lower limit of quantification, where a variation in accuracy of 20% was accepted.

Statistical analysis: Data show the mean ± SEM if not otherwise stated. Statistical analysis was performed by Student's t-test or two-way analysis of variance (ANOVA) with Dunnett`s posthoc test for multiple comparisons if appropriate.

Results

1) SLM6031434 treated mice develop an attenuated fibrotic response after UUO

To investigate the therapeutic potential of SK2 inhibition in tubulointerstitial fibrosis, we tested a novel commercially available highly selective SK2 inhibitor, SLM6031434, and the recently synthesized compound HWG-35D [16] in a mouse model of fibrosis induced by UUO. These two inhibitors have higher selectivity and potencies as compared to previous SK2 inhibitors including ABC294640 and SLP120701 (Table 1).

Mice were treated daily with either vehicle control or with 5 mg/kg SLM6031434 (herein abbreviated SLM) and 7 days after obstruction procedure the fibrotic response in the ligated kidneys was examined. Vehicle-treated mice showed a substantial increase in interstitial fibrosis after 7 days of kidney obstruction. This was demonstrated in PAS (Fig. 1A) and in AZAN stained kidney sections, which show an increased blue staining of collagen fibres (Fig. 1B). In comparison, the deposition of ECM as measure for the degree of fibrosis was much less severe in SLM-treated mice. Quantification of fibrillar collagen in Sirius Red stained sections also confirmed a significant reduction of collagen deposition in UUO kidneys of mice treated with SLM (Fig. 1C, E). Additionally, we performed αSMA staining to evaluate the degree of myofibroblast activation since myofibroblasts are the major drivers of fibrogenesis in the kidney [18]. UUO sections of SLM-treated mice showed a significant reduction in αSMA staining and therefore a lower degree of myofibroblast activation compared to UUO sections of vehicle-treated mice (Fig. 1D, F). Consistent with these results, SLM-treated mice exhibited lower levels of UUO-induced mRNA and protein expression of classic fibrotic markers, such as collagen-1, fibronectin-1, CTGF and αSMA compared to vehicle-treated mice, as measured by quantitative real-time measurements and Western blot analysis (Fig. 1G-I).

Fig. 1: SLM6031434 treatment attenuates fibrotic parameters in UUO

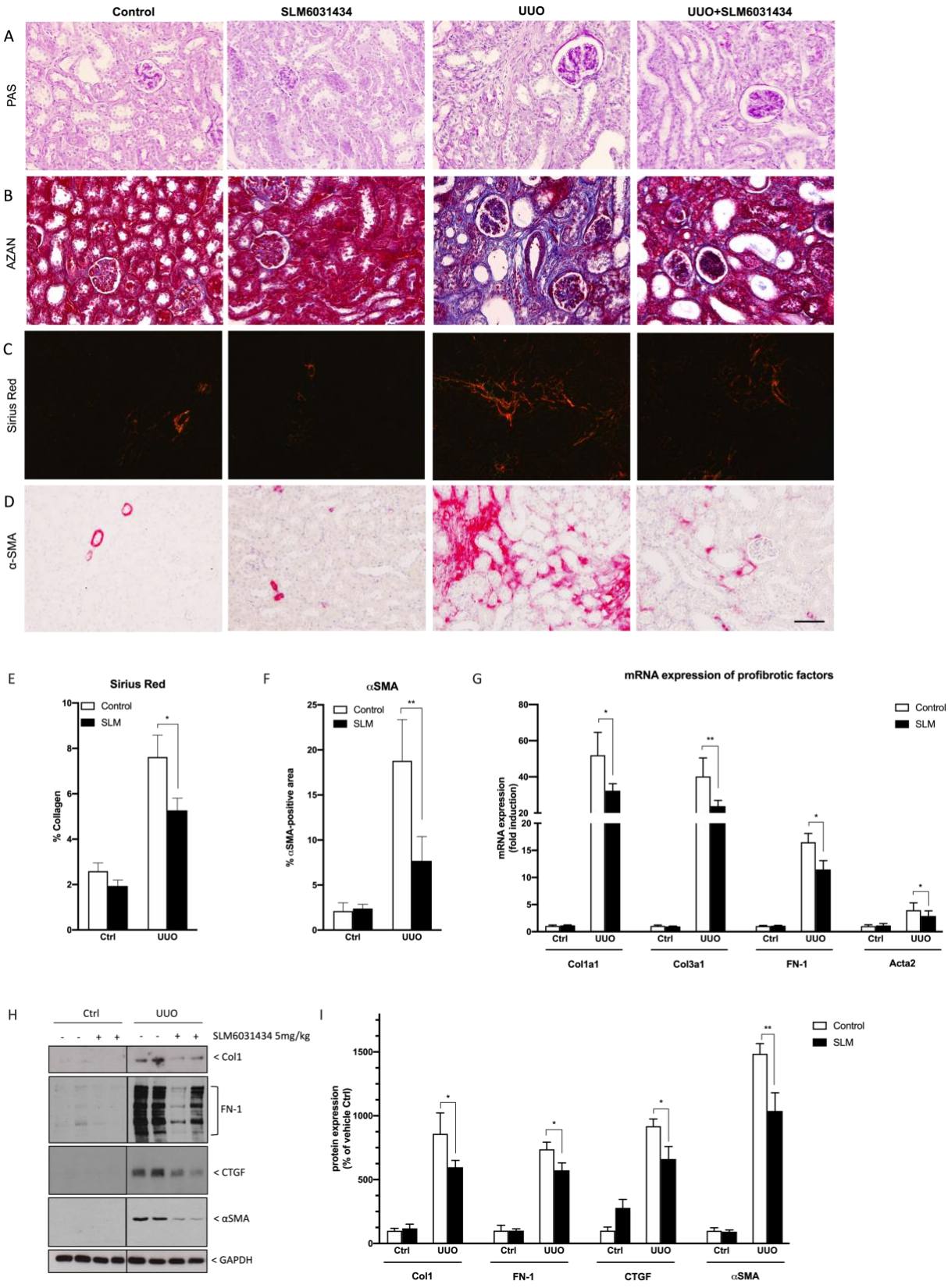

*PAS (A), Azan (B), Sirius Red (C) and α-smooth muscle actin (D, αSMA) staining demonstrating fibrotic changes and myofibroblast activation in representative kidney sections of ligated (UUO) and contralateral (Ctrl) kidneys of vehicle (Control) and SLM6031434 (SLM) treated mice after 7 days (Scale: 50 µm). C) Sirius Red stained sections were photographed under polarized light to detect birefringence of collagen fibres and quantified using ImageJ software. E, F) Graph shows the Collagen quantification of Sirius Red (E) and αSMA (F) stained kidney sections of vehicle-treated (Control, white bars) and SLM-treated (SLM, black bars) mice. (G) RT-qPCR analysis normalized to 18S of collagen 1a1 (Col1a1), Col3a1, fibronectin-1 (FN-1) and Acta-2. H) Representative Western Blots of Col1 (H, upper panel), FN-1 (H, second panel), CTGF (H, third panel) and α-smooth muscle actin (H, α-SMA, forth panel) and I) densitometric analysis of Col1, FN1, CTGF and α-SMA protein expression normalized to GAPDH (H, lower panel) in whole kidney homogenates of ligated (UUO) and contralateral (Ctrl) kidneys at day 7 of vehicle-treated (Control, -, white bars) and SLM-treated (SLM, +, black bars) mice. *p<0.05 and **p<0.01 compared to Control UUO kidneys are considered statistically significant (n=6-10).*

2) HWG-35D-treated mice develop an attenuated fibrotic response after UUO

In addition to SLM6031434, we tested another highly selective and potent SK2 inhibitor, HWG-35D [16] in the UUO model. Since pharmacokinetics data of HWG-35D were not available, equal doses of SLM and HWG-35D were used. Therefore, similar to SLM, mice were intraperitoneally injected daily with either 5 mg/kg of the substance or with vehicle. AZAN and Sirius Red stainings of renal sections revealed that kidneys of HWG-35D-treated mice showed a similar reduction in ECM accumulation and therefore fibrosis to SLM-treated mice as well as a diminished activation of myofibroblast as shown by less αSMA positive staining in IHC (Fig. 2A-E). As expected, also the mRNA and protein expression of Col1, FN-1, CTGF and αSMA measured by quantitative real-time PCR and Western blot analysis were significantly reduced in ligated kidneys of HWG-35D-treated mice in comparison to vehicle-treated controls (Fig. 2F-H). We thereby confirmed with a second compound the protective effect of SK2 inhibition on renal fibrogenesis.

Fig. 2: HWG-35D treatment attenuates fibrotic parameters in UUO

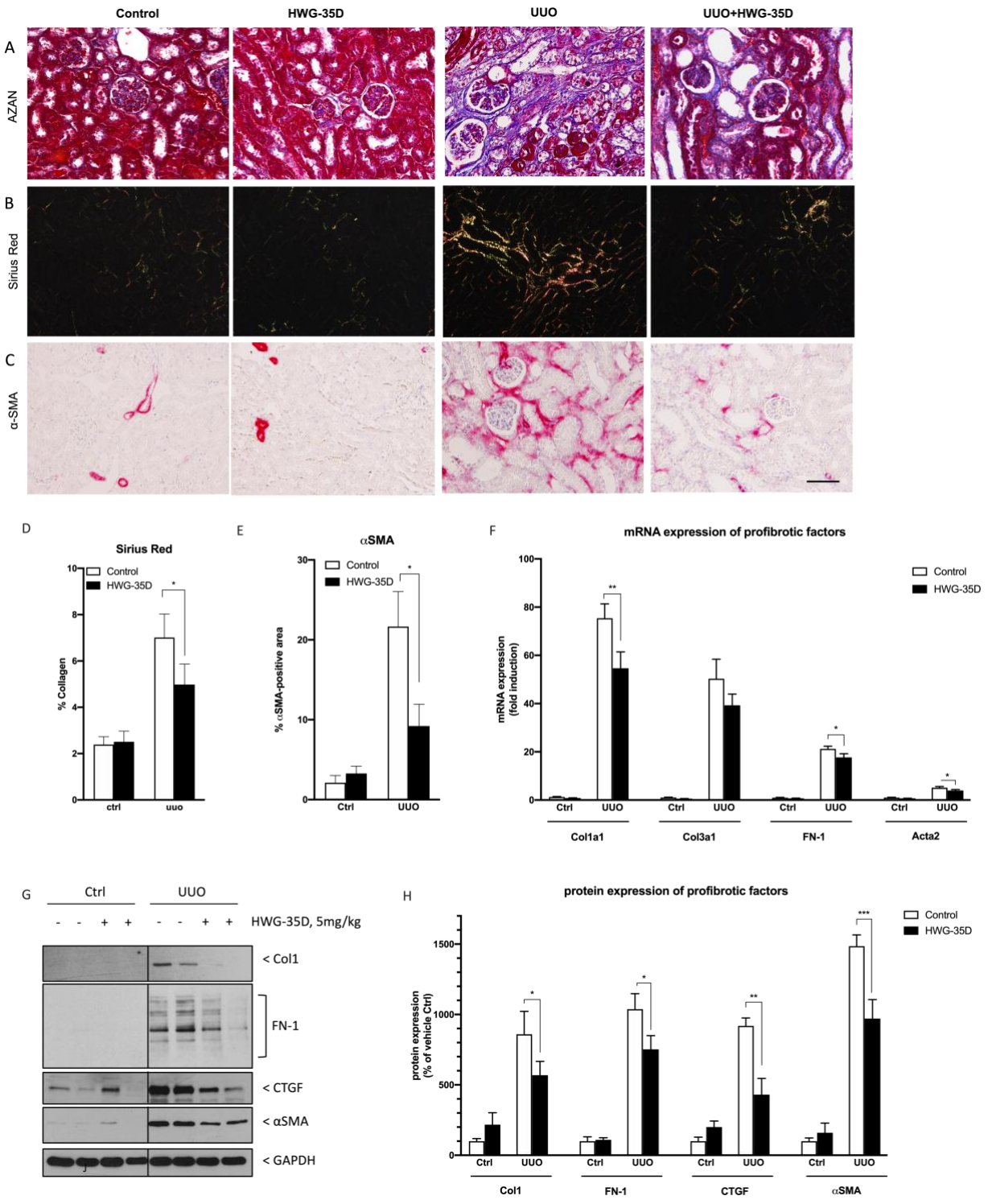

Azan (A), Sirius Red (B) and α-smooth muscle actin (C, αSMA) staining demonstrating fibrotic changes and myofibroblast activation in representative kidney sections of ligated (UUO) and contralateral (Ctrl) kidneys of vehicle (Control) and HWG-35D-treated mice after 7 days (Scale: 50 µM). B) Sirius Red stained sections

*were photographed under polarized light to detect birefringence of collagen fibres and quantified using ImageJ software. D, E) Graphs show the Collagen quantification of Sirius Red (D) and αSMA (E) stained kidney sections of vehicle treated (Control, white bars) and HWG-35D treated (HWG-35D, black bars) mice. (F) RT-qPCR analysis normalized to GAPDH of collagen 1a1 (Col1a1), Col3a1, fibronectin-1 (FN-1) and Acta-2. G) Representative Western Blots of Col1 (G, upper panel), FN-1 (G, second panel), CTGF (G, third panel) and α-smooth muscle actin (G, α-SMA, forth panel) and H) densitometric analysis of Col1, FN1, CTGF and α-SMA protein expression normalized to GAPDH (G, lower panel) in whole kidney homogenates of ligated (UUO) and contralateral (Ctrl) kidneys at day 7 of vehicle-treated (Control, -, white bars) and HWG-35D-treated (HWG-35D, +, black bars) mice. *p<0.05, **p<0.01, ***p<0.001 compared to Control UUO kidneys are considered statistically significant (n=6).*

3) Effect of SK2 inhibition with SLM6031434 and UUO on plasma and kidney tissue sphingosine and S1P levels.

We have concentrated on SLM6031434 for mechanistic studies and performed LC-MS/MS analysis of lipid extractions of plasma and kidney tissue from vehicle and SLM-treated mice to evaluate the effect of SK2 inhibition and UUO on sphingolipid concentration. We focused on the measurement of sphingosine and S1P, as these lipid mediators represent the substrate and the product of SK2. The plasma was collected from mice before (=Ctrl) and 7 days after kidney ligation (=UUO) and plasma sphingosine level substantially increased after UUO in both treatment groups with no significant differences (Fig. 3A). However, in lipid extracts of kidney homogenates, we found a strong increase of tissue sphingosine only in the group treated with the SK2 inhibitor, consistent with inhibition of SK2 (Fig. 3C). Basal plasma S1P levels were already higher in SLM-treated mice, as previously described[19], and resemble the higher basal S1P levels detected in *Sphk2*$^{-/-}$ mice compared to WT mice. UUO led to an even higher increase in plasma S1P, which was not detected in vehicle-treated control mice (Fig. 3B). Similar to tissue sphingosine levels, the S1P concentration also significantly increased in kidney tissue of mice treated with the SK2 inhibitor in comparison to vehicle-treated mice independent of UUO (Fig. 3D). In our previous

study, we demonstrated an association of significantly enhanced Smad7 protein expression with an ameliorated fibrotic response in *Sphk2*$^{-/-}$ mice. Smad7 is a crucial negative regulator of the classic profibrotic TGFβ/Smad signalling cascade by preventing p-Smad2/3 activation. Indeed, similar to the impact of a genetic SK2 deletion in mice, pharmacological SK2 inhibition with SLM resulted in a strong upregulation of Smad7 protein expression, which was further enhanced after kidney obstruction (Fig. 3E, F). In contrast, Smad2 phosphorylation and hence activation was significantly reduced in UUO kidneys of SLM-treated mice (Fig. 3E, F), pointing to a Smad7-dependent downregulation of the TGFβ/Smad signalling pathway.

Fig. 3: Effect of SLM6031434 treatment on plasma and kidney tissue sphingosine and S1P levels, Smad7 expression and Smad2 phosphorylation in UUO kidneys.

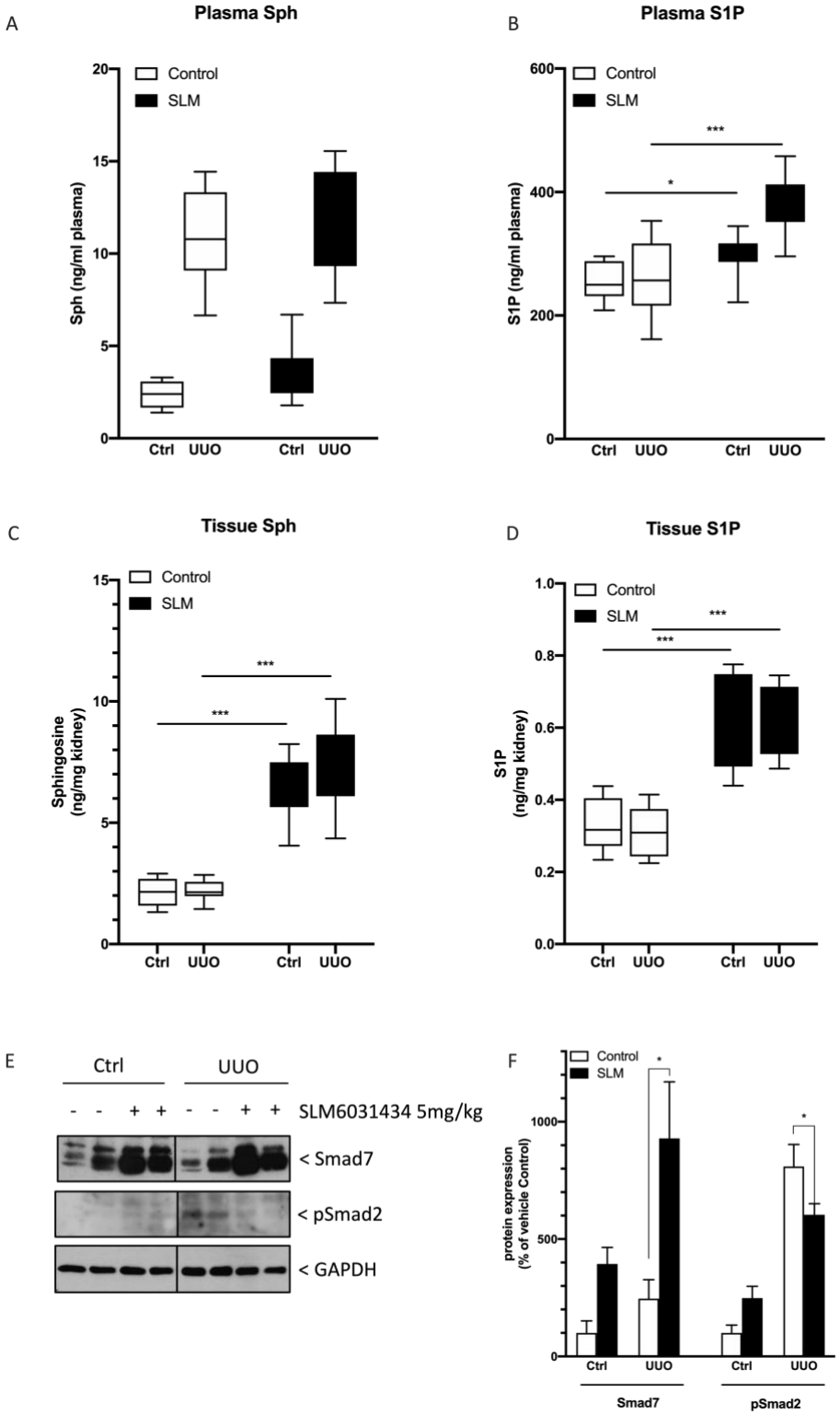

*Plasma sphingosine (A) and S1P (B) levels of vehicle-treated (Control, white boxes) and SLM6031434 (SLM, black boxes) mice before ureteral obstruction procedure (Ctrl) and 7 days after obstruction (UUO) measured by LC-MS/MS after lipid extraction as described in the methods section. Sphingosine (C) and S1P (D) level in lipid extracts of whole kidney homogenates of ligated (UUO) and contralateral kidneys (Ctrl) at day 7 of vehicle-treated (Control, white bars) and SLM-treated (SLM, black bars) mice. Boxplots show the median value, the upper and lower quartile ± minimum and maximum values. (E, F) Densitometric analysis and representative Western blots showing Smad7 (E, upper panel) and phospho-Smad2 (E, pSmad2, second panel), and GAPDH (E, lower panel) of whole kidney homogenates of ligated (UUO) and contralateral kidneys (Ctrl) at day 7 of vehicle-treated (-, white bars) and SLM-treated (+, black bars) mice. *p<0.05, **p<0.01 and ***p<0.001 to Control UUO kidneys are considered statistically significant (n=6-10).*

4) SLM6031434 or HWG-35D treatment differentially regulates Smad7 and CTGF expression in primary kidney fibroblasts.

Activated myofibroblasts are major contributors to disease progression in renal fibrosis [18,20]. We therefore isolated primary kidney fibroblasts from mice and measured the effect of SLM or HWG-35D on TGFβ-induced expression of profibrotic marker proteins. Treatment of cells with TGFβ significantly increased the protein amount of CTGF and FN-1 (Fig. 4A, D). However, pre-treatment of fibroblasts with 3 µM of SLM or HWG-35D resulted in a clear reduction of TGFβ-induced CTGF, FN-1 and Col1 expression. Additionally, we tested the effect of both SK2 inhibitors on Smad7 expression and indeed detected a dose-dependent increase of Smad7 protein expression in SK2 inhibitor-treated fibroblast (Fig. 4B, C, E, F).

Fig. 4: Effect of SLM6031434 or HWG-35D on TGFβ-induced profibrotic marker and Smad7 protein expression in primary murine fibroblasts.

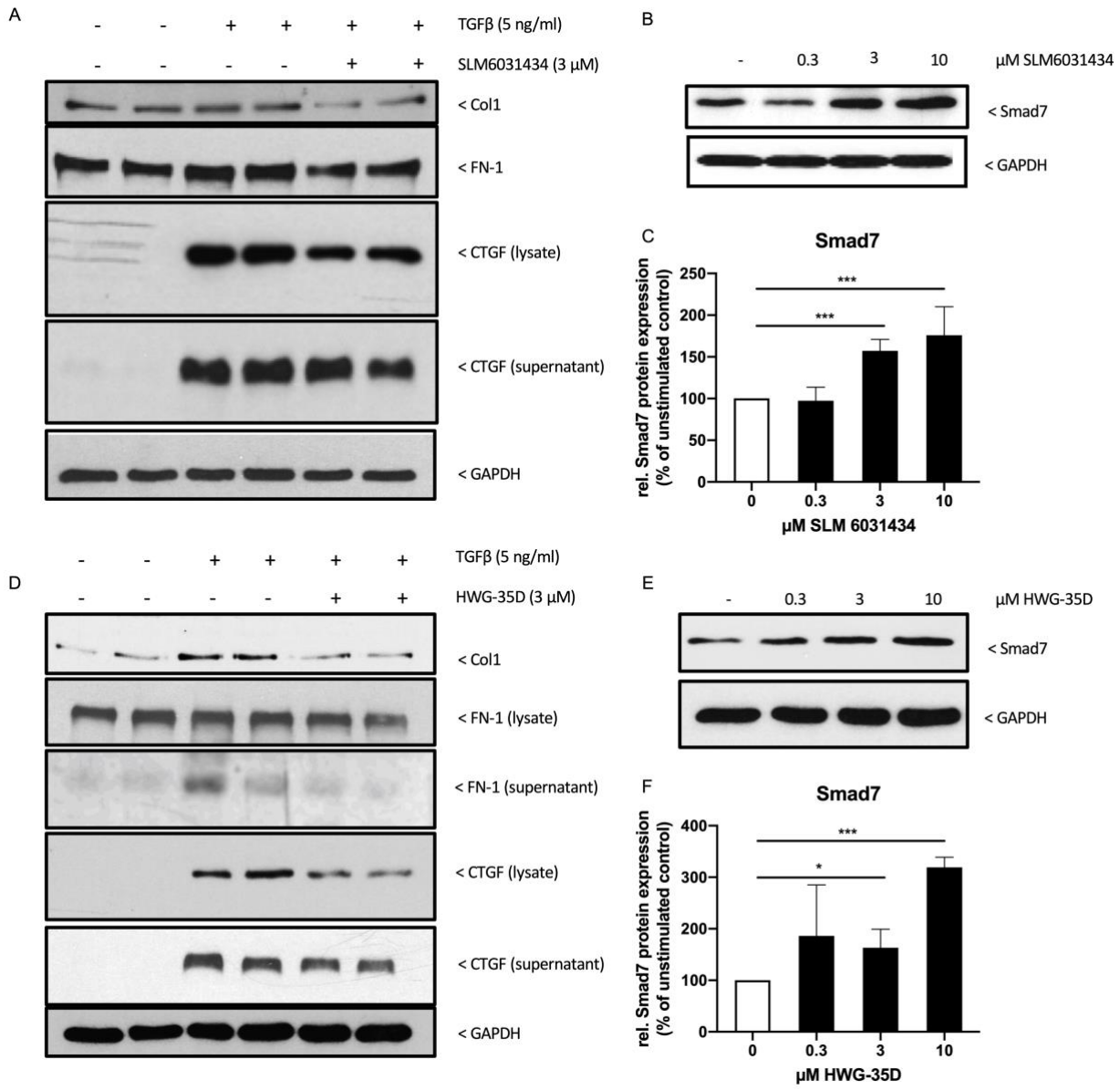

A, D) Representative Western blots showing Col1, FN-1 in cell lysates and CTGF and FN-1 protein expression in supernatants and cell lysates of quiescent primary kidney fibroblasts, which were stimulated with TGFβ (5 ng/mL) in the absence (-) or presence (+) of SLM6031434 (A, 3 µM, pre-incubation for 16 h) or HWG-35D (D, 3 µM, pre-incubation for 16 h) for 6 h. B-C, E-F) Representative Western blot (B, E) and densitometric analysis (C, F) showing Smad7 (upper panel) and GAPDH (lower panel) in primary kidney fibroblasts after treatment for 16 h with the indicated concentration of SLM6031434 (B, C) or HWG-35D (E,

*F). Data in (C and F) show the mean ± SD of Western blots of 3 independent experiments. *p<0.05 and ***p<0.001 are considered statistically significant to unstimulated controls.*

5) Effect of SLM6031434 treatment on IFNγ, M1- and M2-type macrophage marker expression

Other studies in which the protective role of an SK2 deficiency in renal fibrosis has been investigated, suggested an upregulation of IFNγ[14], or an enhancement of anti-inflammatory M2-macrophage population[15] as the responsible mechanism. We therefore measured the mRNA expression of IFNγ, iNOS (as an M1-type macrophage marker) and Mcr1/CD206 (as an M2-type macrophage marker). As seen in Fig. 5A, we could not detect a renal upregulation of IFNγ mRNA expression in UUO upon SK2 inhibition by SLM treatment. The expression levels of iNOS and Mcr1/CD206 were both significantly reduced in SLM-treated ligated kidneys (Fig. 5 B, C). Based on these results, we did not observe an upregulation of M2 macrophages and rather expect a reduction in total macrophage numbers in the inhibitor-treated obstructed kidneys. For this reason, we further evaluated ligation-induced macrophage infiltration in the tubular interstitium by performing IHC using a F4/80 antibody. Although both treatment groups showed an increased F4/80 positive staining upon kidney obstruction, the substantial infiltration of macrophages detected in vehicle-treated control mice was significantly attenuated in SLM-treated mice (Fig. 5D, E), thereby reflecting the reduced mRNA expression of macrophage markers in these kidneys.

Fig. 5: Effect of SK2 inhibition and UUO on Interferon-γ, iNOS and Mcr-1 mRNA expression and macrophage infiltration.

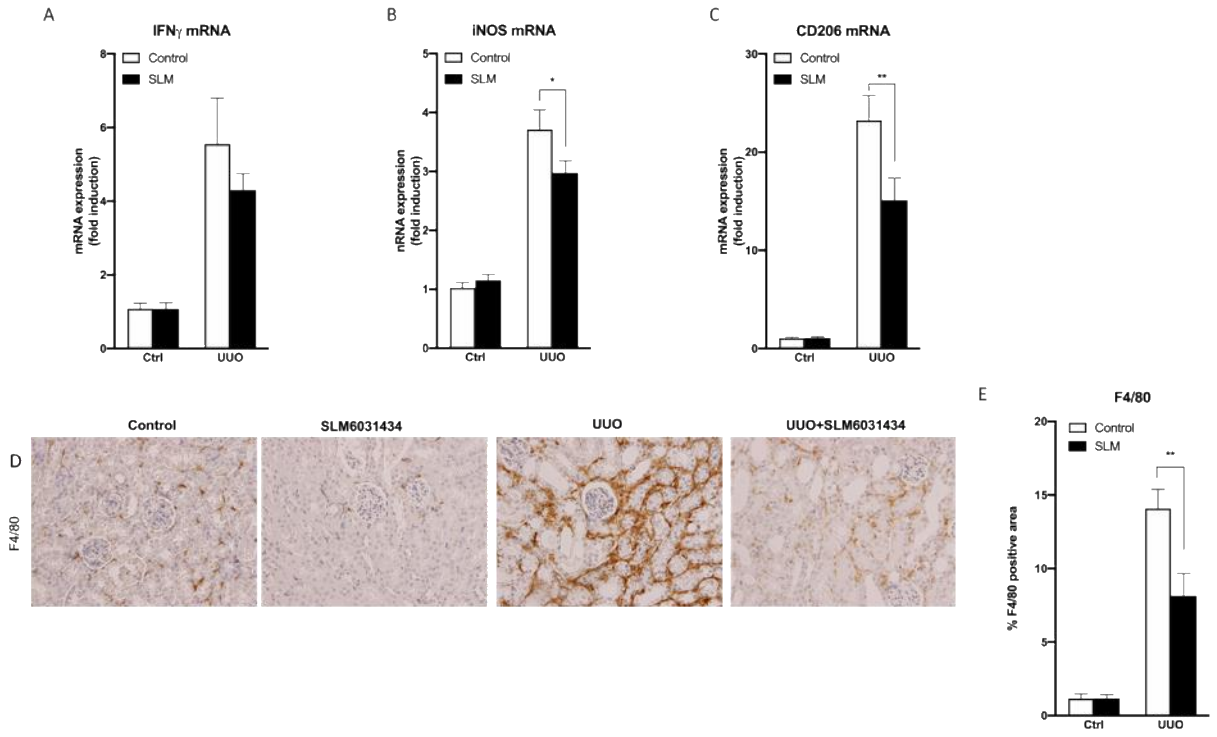

(A-C) RT-qPCR analysis normalized to 18S of interferon-γ (A, IFNγ), iNOS (B) and Mcr1 (C) in whole kidney homogenates of ligated (UUO) and contralateral kidneys (Ctrl) at day 7 of vehicle-treated (Control, white bars) and SLM6031434-treated (SLM, black bars) mice (n=6-10).

*(D, E) F4/80 staining (D) and quantification (E) demonstrating macrophage infiltration in representative kidney sections of ligated (UUO) and contralateral (Ctrl) kidneys of vehicle (Control, white bars) and SLM6031434 (SLM, black bars) treated mice after 7 days (Scale: 100 µM). **p<0.01 compared to Control UUO kidneys is considered statistically significant (n=6-10).*

Discussion

In this study we have validated two highly selective SK2 inhibitors for therapeutic use as anti-fibrotic agents in a mouse model of tubulointerstitial fibrosis. Previously, we and others have shown that SK2 serves as an attractive novel target to treat renal fibrosis. By using SK2-deficient mice, tubulointerstitial fibrosis, induced by either ureter ligation (UUO) [12,13] or folic acid administration [14], was reduced as compared to wildtype mice. However, no consensus about the underlying mechanism can be drawn from these different studies. While Bajwa et al. suggested

393 an upregulation of IFNγ production as the main protective mechanism [14], this was not seen by
394 Schwalm et al., who rather suggested the upregulation of the anti-fibrotic Smad7 as a key factor
395 mediating protection [12,13]. Notably, IFNγ, as well as its receptors IFNγR1 and R2, were found to be
396 upregulated in wildtype UUO and *Sphk2*$^{-/-}$ UUO mice in a comparable manner [12]. Nevertheless,
397 IFNγ can have anti-fibrotic potential as reported by administration of recombinant IFNγ, or an IFNγ
398 peptidomimetic, which both dampened the fibrotic response in UUO mice [21,22].
399 In another study, Ghosh et al. [15] proposed that loss of SK2 triggers a switch in macrophage
400 polarization towards the anti-inflammatory and more healing M2 macrophages at the expense of
401 pro-inflammatory M1 macrophages. However, in the present study we did not detect an
402 upregulation of either IFNγ or of the M2 macrophage marker expression Mcr1/CD206 in obstructed
403 kidneys upon SK2 inhibition. These discrepancies might be caused by the use of different kidney
404 fibrosis models or by the selection of different time points to study macrophage infiltration. A third
405 mechanism was proposed by Zhu et al. [13], who showed that in UUO, SK2 directly binds and
406 activates Fyn which leads to Akt and STAT3 activation and subsequent fibroblast activation.
407 Consequently, blocking SK2 resulted in reduced myofibroblast activation and ECM production. In
408 summary, all these data suggest that pharmacological inhibition of SK2 should have a beneficial
409 effect in renal fibrosis whatsoever the precise mechanism might be.
410 Regarding the impact of SK2 inhibition on sphingolipid concentration, we expectedly observed an
411 SLM-induced accumulation of the SK2 substrate sphingosine in renal tissue regardless of the
412 obstruction procedure. As previously shown, sphingosine contributes to the anti-fibrotic effect in
413 *Sphk2-/-* mice by upregulating Smad7 protein expression[12] which very likely occurs upon SK2
414 inhibitor treatment as well. Surprisingly, tissue S1P levels were also higher in kidneys of SLM-
415 treated mice. It is possible that accumulation of sphingosine caused by SK2 inhibition is used by
416 SK1 to make more S1P and this pool of S1P is specifically protective in the UUO model. This
417 hypothesis is in line with other studies that demonstrate a protective role for SK1 in kidney injury
418 models [9–11]. However, the concentration of tissue S1P is very low and we cannot exclude a

419 contamination of kidney tissue with minor amounts of blood which contains higher S1P levels in
420 SLM-treated mice [19].
421
422 Although a number of inhibitors of SK2 have been described to date, selectivity and potency with
423 early compounds is typically modest (Table 1) and it is only very recently that highly selective and
424 potent SK2 inhibitors have emerged as tool compounds for exploring pharmacological inhibition
425 of SK2. As compared to first generation inhibitors of SKs, such as dimethylsphingosine (DMS) and
426 SKI-II [23], which exhibit no selectivity between SK1 and SK2, second generation SK2 inhibitors
427 have been developed that show improved selectivity and potency. Among these is ABC294640
428 [24], a compound that has several-fold selectivity for SK2 over SK1. However, the potency of
429 ABC294640 remains relatively poor with an *in vitro* IC_{50} value for SK2 at 60 μM and a cellular IC_{50}
430 value at 26 μM [24]. Notwithstanding these apparently disadvantageous parameters for further
431 development, the inhibitor has nevertheless proved efficacious in various mouse tumor models
432 and reduces tumor growth significantly [25,26]. Moreover, ABC294640 (Opaganib, Yeliva^R) has
433 recently successfully passed clinical trials in patients with diffuse large B cell lymphoma and
434 multiple myeloma, and is now FDA approved with orphan drug status for the treatment of
435 cholangiocarcinoma. ABC294640 has also been tested in UUO mice and was able to reduce
436 fibrosis [13] although extremely high concentrations of 50mg/kg/day were needed, which makes
437 translation into human difficult. Even more promising than ABC294640 is the newly developed
438 selective SK2 inhibitor SLP120701 [27], which possesses an IC_{50} value for SK2 of 1.2 μM and an 8-
439 10-fold selectivity for SK2 over SK1. In the UUO model, Ghosh et al. showed that SLP120701
440 diminished UUO-induced renal injury and fibrosis [15].
441 In our study, we have now included two even more selective SK2 inhibitors (Table 1) of even
442 higher potencies, i.e. SLM6031434 [19] and HWG-35D [16]. While SLM6031434 has an IC_{50} value for
443 SK2 of 400 nM and is approx. 40-fold more selective for SK2 than SK1, HWG-35D has an even
444 lower IC_{50} value of 41 nM and a selectivity factor of >100-fold over SK1 [16]. Both of these

compounds mediated a protection from UUO-induced renal fibrosis. Therefore, further development SK2 inhibitors as a new drug class seems very promising and is warranted because, to date, an efficient treatment of renal fibrosis is still missing. So far, treatment aims are to reduce the preceding inflammatory phase of interstitial nephritis by glucocorticoids, or to minimise risk factors of chronic kidney disease such as hypertension and diabetes. However, glucocorticoids are well known to couple to a series of unwanted adverse effects [28], that make their use as a therapeutic option, particularly for chronic conditions, less attractive for the patient.

Adverse effects that arise from inhibition of SK2 are still poorly explored. However, since a role for SK2 in platelet aggregation was reported [29], alteration in blood coagulation must be kept in mind. In this regard, *ex vivo* isolated platelets from *Sphk2*-deficient mice showed an impaired aggregation upon PAR4-P and ADP stimulation, which was based on a defective thromboxane A2 release [29]. Furthermore, SK2 is hypothesized to have a protective role in stroke, and thus, *vice versa*, depletion of SK2 led to increased ischemic lesion size and worsened neurological function in a stroke model in mice [30]. If indeed, SK2 inhibition leads to an increased risk of stroke, this certainly would be a severe adverse effect that may have considerable impact on a further development of such compounds. However, any phenotype seen in *Sphk2*-deficient mice may not necessarily occur upon SK2 inhibitor treatment because the inhibitor is only given for a restricted time period and long-term adaptive processes may not become evident.

In summary, our data demonstrate that that two highly selective and potent SK2 inhibitors are effective in reducing a fibrotic response and renal injury in a mouse model. Thus, we conclude that SK2 is a valid pharmacological target for reducing renal inflammation and fibrosis. Whether this protective effect of SK2 inhibition is of a more general nature and also occurs in other organs undergoing fibrosis, is presently unclear, but clearly warrants further investigation.

Table 1: Comparison of SK2 inhibitors in terms of selectivity and potency

Compound	IC_{50} for SK2	IC_{50} for SK1	Selectivity factor SK2/SK1	Reference
ABC294640	60 μM	>100 μM	>1.6x	French et al., 2010 [24]
SLP120701	1.2 μM	>10 μM	>8x	Patwardhan et al., 2015 [27]
SLM6031434	0.4 μM	16 μM	40x	Kharel et al., 2015 [19]
HWG-35D	0.041 μM	4.1 μM	100x	Adams et al., 2019 [16]

471

472

473 **Author contributions**

474 S.S. – Investigation, Methodology, Visualization, Writing – Original Draft, Project administration

475 S.B. – Investigation

476 R.H. – Investigation

477 S.T. – Investigation

478 G.G. – Project administration

479 D.A. – Resources

480 S.P. and N.P. – Resources, Writing – Review & Editing

481 L.S. – Data curation, Funding acquisition

482 A.H. – Conceptualization, Project administration, Funding acquisition, Writing – Original Draft

483 J.P. – Conceptualization, Project administration, Funding acquisition, Writing – Review & Editing

484

485 **Funding**

486 This work was supported by the German Research Foundation (SFB1039 TPB02, TPZ01, SFB

487 1177, project E2) and the Swiss National Science Foundation (310030_135619).

488

489 **Acknowledgement**

We thank Simone Albert and Isolde Römer for excellent technical assistance.

Disclosure

All the authors declare no competing interest.

References

1. Foreman KJ, Marquez N, Dolgert A, et al. Forecasting life expectancy, years of life lost, and all-cause and cause-specific mortality for 250 causes of death: reference and alternative scenarios for 2016–40 for 195 countries and territories. *Lancet*. 2018;392(10159):2052-2090. doi:10.1016/S0140-6736(18)31694-5
2. Hla T, Dannenberg AJ, Aerts JM, et al. Sphingolipid signaling in metabolic disorders. *Cell Metab*. 2012;16(4):420-434. doi:10.1016/j.cmet.2012.06.017
3. Maceyka M, Harikumar KB, Milstien S, Spiegel S. Sphingosine-1-phosphate signaling and its role in disease. *Trends Cell Biol*. 2012;22(1):50-60. doi:10.1016/j.tcb.2011.09.003
4. Schwalm S, Pfeilschifter J, Huwiler A. Sphingosine-1-phosphate: A Janus-faced mediator of fibrotic diseases. *Biochim Biophys Acta - Mol Cell Biol Lipids*. 2013;1831(1):239-250.
5. Pyne NJ, Dubois G, Pyne S. Role of sphingosine 1-phosphate and lysophosphatidic acid in fibrosis. *Biochim Biophys Acta - Mol Cell Biol Lipids*. 2013;1831(1):228-238. doi:10.1016/j.bbalip.2012.07.003
6. Huwiler A, Pfeilschifter J. Sphingolipid signaling in renal fibrosis. *Matrix Biol*. 2018;68-69:230-247. doi:10.1016/j.matbio.2018.01.006
7. Xin C, Ren S, Kleuser B, et al. Sphingosine 1-phosphate cross-activates the Smad signaling cascade and mimics transforming growth factor-beta-induced cell responses. *J Biol Chem*. 2004;279(34):35255-35262. doi:10.1074/jbc.M312091200
8. Alemany R, van Koppen CJ, Danneberg K, Ter Braak M, Meyer Zu Heringdorf D. Regulation and functional roles of sphingosine kinases. *Naunyn Schmiedebergs Arch*

Pharmacol. 2007;374(5-6):413-428. doi:10.1007/s00210-007-0132-3

9. Du C, Ren Y, Yao F, et al. Sphingosine kinase 1 protects renal tubular epithelial cells from renal fibrosis via induction of autophagy. *Int J Biochem Cell Biol*. 2017;90:17-28. doi:10.1016/j.biocel.2017.07.011

10. Ren S, Babelova A, Moreth K, et al. Transforming growth factor-beta2 upregulates sphingosine kinase-1 activity, which in turn attenuates the fibrotic response to TGF-beta2 by impeding CTGF expression. *Kidney Int*. 2009;76(8):857-867. doi:10.1038/ki.2009.297

11. Natoli TA, Husson H, Rogers KA, et al. Loss of GM3 synthase gene, but not sphingosine kinase 1, is protective against murine nephronophthisis-related polycystic kidney disease. *Hum Mol Genet*. 2012;21(15):3397-3407. doi:10.1093/hmg/dds172

12. Schwalm S, Beyer S, Frey H, et al. Sphingosine Kinase-2 Deficiency Ameliorates Kidney Fibrosis by Up-Regulating Smad7 in a Mouse Model of Unilateral Ureteral Obstruction. *Am J Pathol*. 2017;187(11). doi:10.1016/j.ajpath.2017.06.017

13. Zhu X, Shi D, Cao K, et al. Sphingosine kinase 2 cooperating with Fyn promotes kidney fibroblast activation and fibrosis via STAT3 and AKT. *Biochim Biophys Acta - Mol Basis Dis*. 2018;1864(11):3824-3836. doi:10.1016/j.bbadis.2018.09.007

14. Bajwa A, Huang L, Kurmaeva E, et al. Sphingosine Kinase 2 Deficiency Attenuates Kidney Fibrosis via IFN-γ. *J Am Soc Nephrol*. Published online October 31, 2016:ASN.2016030306. doi:10.1681/ASN.2016030306

15. Ghosh M, Thangada S, Dasgupta O, et al. Cell-intrinsic sphingosine kinase 2 promotes macrophage polarization and renal inflammation in response to unilateral ureteral obstruction. Long D, ed. *PLoS One*. 2018;13(3):e0194053. doi:10.1371/journal.pone.0194053

16. Adams DR, Tawati S, Berretta G, et al. Topographical Mapping of Isoform-Selectivity Determinants for J-Channel-Binding Inhibitors of Sphingosine Kinases 1 and 2. Published online 2019. doi:10.1021/acs.jmedchem.9b00162

17. Nakagawa N, Yuhki K, Kawabe J, et al. The intrinsic prostaglandin E2–EP4 system of the renal tubular epithelium limits the development of tubulointerstitial fibrosis in mice. *Kidney Int*. 2012;82(2):158-171. doi:10.1038/ki.2012.115
18. Duffield JS. Cellular and molecular mechanisms in kidney fibrosis. *J Clin Invest*. 2014;124(6):2299-2306. doi:10.1172/JCI72267
19. Kharel Y, Morris EA, Congdon MD, et al. Sphingosine Kinase 2 Inhibition and Blood Sphingosine 1-Phosphate Levels. *J Pharmacol Exp Ther J Pharmacol Exp Ther*. 2015;355:23-31. doi:10.1124/jpet.115.225862
20. Strutz F, Zeisberg M. Renal fibroblasts and myofibroblasts in chronic kidney disease. *J Am Soc Nephrol*. 2006;17(11):2992-2998. doi:10.1681/ASN.2006050420
21. Oldroyd SD, Thomas GL, Gabbiani G, El Nahas AM. Interferon-γ inhibits experimental renal fibrosis. *Kidney Int*. 1999;56(6):2116-2127. doi:10.1046/j.1523-1755.1999.00775.x
22. Poosti F, Bansal R, Yazdani S, et al. Interferon gamma peptidomimetic targeted to interstitial myofibroblasts attenuates renal fibrosis after unilateral ureteral obstruction in mice. *Oncotarget*. 2016;7(34):54240-54252. doi:10.18632/oncotarget.11095
23. Santos WL, Lynch KR. Drugging sphingosine kinases. *ACS Chem Biol*. 2015;10(1):225-233. doi:10.1021/cb5008426
24. French KJ, Zhuang Y, Maines LW, et al. Pharmacology and antitumor activity of ABC294640, a selective inhibitor of sphingosine kinase-2. *J Pharmacol Exp Ther*. 2010;333(1):129-139. doi:10.1124/jpet.109.163444
25. Antoon JW, White MD, Meacham WD, et al. Antiestrogenic Effects of the Novel Sphingosine Kinase-2 Inhibitor ABC294640. *Endocrinology*. 2010;151(11):5124-5135. doi:10.1210/en.2010-0420
26. Antoon JW, White MD, Slaughter EM, et al. Targeting NFκB mediated breast cancer chemoresistance through selective inhibition of sphingosine kinase-2. *Cancer Biol Ther*. 2011;11(7):678-689. doi:10.4161/cbt.11.7.14903

27. Patwardhan NN, Morris EA, Kharel Y, et al. Structure-activity relationship studies and in vivo activity of guanidine-based sphingosine kinase inhibitors: Discovery of SphK1- and SphK2-selective inhibitors. *J Med Chem*. 2015;58(4):1879-1899. doi:10.1021/jm501760d

28. Ponticelli C, Locatelli F. Glucocorticoids in the treatment of glomerular diseases: Pitfalls and pearls. *Clin J Am Soc Nephrol*. 2018;13(5):815-822. doi:10.2215/CJN.12991117

29. Urtz N, Gaertner F, von Bruehl M-L, et al. Sphingosine 1-Phosphate Produced by Sphingosine Kinase 2 Intrinsically Controls Platelet Aggregation In Vitro and In VivoNovelty and Significance. *Circ Res*. 2015;117(4).

30. Pfeilschifter W, Czech-Zechmeister B, Sujak M, et al. Activation of sphingosine kinase 2 is an endogenous protective mechanism in cerebral ischemia. *Biochem Biophys Res Commun*. 2011;413(2):212-217. doi:10.1016/j.bbrc.2011.08.070